

## Spin crossover transition in the cluster compounds $\text{Nb}_6\text{I}_{11}$ and $\text{HNb}_6\text{I}_{11}$

J. J. Finley, R. E. Camley, E. E. Vogel,\* V. Zevin,<sup>†</sup> and E. Gmelin  
*Max-Planck-Institut für Festkörperforschung, 7000 Stuttgart 80, Federal Republic of Germany*

(Received 5 December 1980)

Our specific-heat measurements in  $\text{Nb}_6\text{I}_{11}$  indicate a phase transition (PT) at 274 K. Independent x-ray studies confirm that at  $T_c$  a structural phase transition occurs. In  $\text{HNb}_6\text{I}_{11}$  the equivalent PT occurs at 324 K. The magnetic-susceptibility measurements indicate that the electronic ground-state degeneracy of the cluster is reduced by the PT, going from a high-temperature quartet to a doublet for  $\text{Nb}_6\text{I}_{11}$ , and from a high-temperature triplet to a singlet for  $\text{HNb}_6\text{I}_{11}$ . Independent band-structure calculations suggest that, in distinction to the cooperative Jahn-Teller effect, the ground-level degeneracy is removed here by the crossing of the electronic levels which start to move with the onset of the structural deformation. The mean-field theory for the susceptibility of a two-level-model system is presented here and fitted to the experiment.

### I. INTRODUCTION

Both  $\text{Nb}_6\text{I}_{11}$  and  $\text{HNb}_6\text{I}_{11}$  belong to a family commonly referred to as cluster compounds.<sup>1</sup> In these compounds the Nb atoms cluster together, forming an octahedron. The interatomic distance of these atoms is close to that of the pure metal indicating covalent bonding. The six metal atoms are surrounded by nonmetal I atoms. The bonding between the nonmetal and metal atoms is primarily covalent, but electronic charge is transferred from the niobium to the iodine ions which helps to hold the cluster together. The lack of saturation of the bonds as well as the low-site symmetry leads to departures from octahedral symmetry.

It has been possible to prepare cluster compounds with octahedra defined by transition metals and rare earths.<sup>2</sup> The nonmetal ions are halogens and chalcogens. These materials form a large and diverse family of unusual compounds providing a vast field of research of their physical properties.<sup>3,4</sup>

The cluster compounds  $\text{Nb}_6\text{I}_{11}$  and  $\text{HNb}_6\text{I}_{11}$ , first prepared and analyzed by Bateman *et al.*,<sup>5</sup> Simon *et al.*,<sup>6</sup> and Simon,<sup>7</sup> show some interesting and unusual physical properties. The first measurements of the magnetic susceptibility in  $\text{Nb}_6\text{I}_{11}$  (Ref. 6) revealed two Curie-Weiss regions, with a large effective magnetic moment at high temperatures and a small effective magnetic moment at lower temperatures. In  $\text{HNb}_6\text{I}_{11}$ ,<sup>7</sup> there is an approximately Curie-Weiss region at high temperature and diamagnetic behavior at low temperature.

One might think this magnetic behavior could be explained by a phenomenological rigid two-level system [ground level  $S = \frac{1}{2}$  and first excited level  $S = \frac{3}{2}$  for  $\text{Nb}_6\text{I}_{11}$  (Ref. 6) and a ground level  $S = 0$  and first excited level  $S = 1$  for  $\text{HNb}_6\text{I}_{11}$  with an intersystem

exchange interaction]. However this model fails to explain the peculiar behavior of the susceptibility between the high- and low-temperature regions.

Recent x-ray measurements<sup>8</sup> have shown that at the temperatures where the susceptibility is rapidly changing a structural phase transition (PT) occurs (apparently of second order). This PT removes the only symmetry element—the center of inversion—of the  $\text{Nb}_6\text{I}_{11}$  cluster.

This deformation behavior coupled with the magnetic-susceptibility measurements mentioned above led us and Nohl and Anderson to believe that the onset of the deformation is accompanied by shifts in the electronic levels. Band-structure calculations by Nohl and Andersen showed the interesting and surprising result that the high-temperature phase of  $\text{Nb}_6\text{I}_{11}$  has a ground state  $S = \frac{3}{2}$  and the low-temperature phase of  $\text{Nb}_6\text{I}_{11}$  has a *different* ground state of  $S = \frac{1}{2}$ . To be consistent with the magnetic measurements, we concluded that in  $\text{HNb}_6\text{I}_{11}$  the high-temperature phase has a ground state of  $S = 1$ , and the low-temperature phase had a ground state of  $S = 0$ . In the region of the PT, these two levels cross. This picture of the phase transition is in full agreement with the recent calculations<sup>9</sup> of the electronic structure and magnetic properties of these compounds.

To the best of our knowledge, this is the first observation of a structural PT in a cluster compound<sup>10</sup> in which the electronic degeneracy is reduced by the crossing of electronic levels.<sup>4</sup> This type of phase transition is analogous to the usual cooperative Jahn-Teller (JT) effect<sup>11</sup> in that in both cases, the reduction of the degeneracy is accompanied by a structural PT. However, instead of a splitting of the degenerate levels as in the usual Jahn-Teller effect, here a level crossing occurs.

It is worthwhile to note that our PT cannot be explained by the usual JT mechanism for the following reason. In general, the JT effect occurs when high symmetry allows the existence of degenerate states. Then the system prefers to lower the symmetry in order to remove the electronic degeneracy. Here there is only very low symmetry at high temperatures (only center of inversion is present even at high temperatures), and the cluster prefers the high-spin ground state at high temperature due to the exchange intra-cluster interaction (a kind of Hund's rule). (The more degenerate high-spin state is also preferred at high temperature by entropy considerations.) Therefore, the only way to remove degeneracy here is to move the one-electron levels in such a manner that the maximum compensation of the spin state occurs.

In this paper we report new studies of the magnetic susceptibility and specific heat for  $\text{Nb}_6\text{I}_{11}$  and  $\text{HNb}_6\text{I}_{11}$  and develop the mean-field theory for the magnetic susceptibility. A brief summary of this work has been presented previously.<sup>4</sup>

We do not discuss in detail the electronic resistivity of these cluster compounds. This will be dealt with in a forthcoming paper. We note only that recent measurements<sup>12</sup> indicate that  $\text{Nb}_6\text{I}_{11}$  is a *n*-type semiconductor. The gap for  $T < T_c$  is approximately 0.40 eV. The conductivity shows a change in slope at  $T_c$  and for  $T > T_c$ , the gap is approximately 0.12 eV.

## II. STRUCTURE AND STRUCTURAL PHASE TRANSITION

In this section we review results of the x-ray structural studies of the  $\text{Nb}_6\text{I}_{11}$  and  $\text{HNb}_6\text{I}_{11}$ .<sup>6-8</sup> The building block,  $\text{Nb}_6\text{I}_8$ , forms a distorted cube with I atoms at the corners and Nb atoms at the face centers. The Nb atoms thus form a distorted octahedron. There are six additional I atoms located approximately on the perpendiculars of the cube faces which are shared between two neighboring  $\text{Nb}_6\text{I}_8$  clusters and provide the intercluster bonding. The structure is illustrated in Fig. 1. The formula unit  $\text{Nb}_6\text{I}_{11}$  therefore corresponds to  $(\text{Nb}_6\text{I}_8)\text{I}_{6/2}$ . The crystal structure is orthorhombic with four clusters per primitive cell. This is schematically shown in Fig. 2. The structure of  $\text{HNb}_6\text{I}_{11}$  is essentially the same, with the H atom located in the center of the octahedron.

The high-temperature phase of  $\text{Nb}_6\text{I}_{11}$  belongs to the *Pccn* space group. In Fig. 2, the  $\text{Nb}_6\text{I}_{11}$  structure may be seen as composed of two families of cluster chains along  $(a, 0, c)$  and  $(-a, 0, c)$  directions. These chains are coupled mainly via two iodine ions which connect two clusters shifted each relative to the other in the  $(a/2, b/2, 0)$  direction. At  $T_c = 274$  K, the structural PT takes place in which the center of inversion is lost. The new phase for  $T < T_c$  belongs to

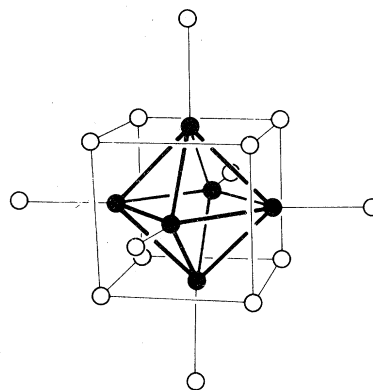


FIG. 1. Structure of a  $\text{Nb}_6\text{I}_{11}$  cluster. The Nb atoms form a distorted octahedra surrounded by a cube with iodine atoms at the corners.

the orthorhombic *P2<sub>1</sub>cn* space group. The cell dimensions do not change essentially (less than 1%), but the deformation of the cluster is large. The deformation may be represented in a crude way as a twist of  $7^\circ$  between the two opposite triangular faces of the Nb octahedron.

The temperature dependence of this deformation may be seen in the temperature dependence (corrected for the effect of thermal vibrations) of the square root of the average intensities,  $\sqrt{I}$ , of the new reflec-

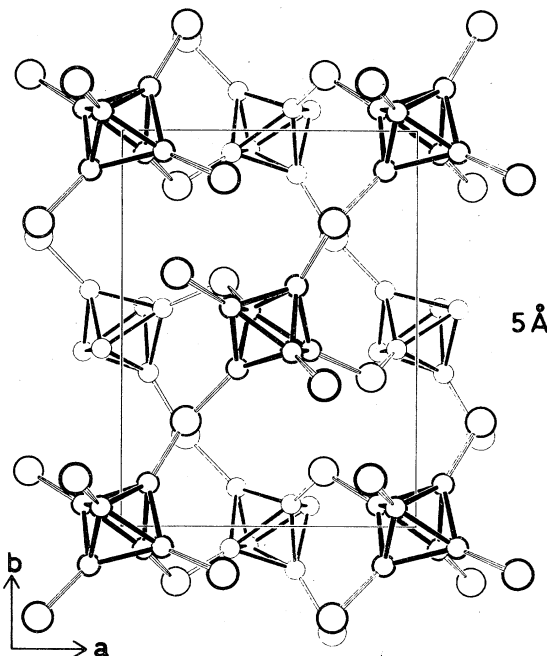


FIG. 2. Structure of the unit cell. For simplicity, the I atoms forming a cube around the Nb octahedra are not shown.

tions which appear due to a change in space group. Figure 3(a) reproduces the results of Imoto and Simon<sup>8</sup> for  $\sqrt{I}$  versus temperature. Inspection of Fig. 3 shows that the transition is very likely of second order. However, a small-jump first-order transition is not excluded by the x-ray analysis. The solid curve in Fig. 3 is the equation

$$\sqrt{I} = \left( \frac{T_c - T}{T_c - T_s} \right)^\beta, \quad T_s < T < T_c, \quad (1)$$

and gives a reasonable approximation to the experimental points especially near  $T_c$  with  $\beta=0.2$  and the saturation temperature  $T_s=156$  K.

Because we expect that  $\sqrt{I}$  is proportional to the deformation, Eq. (1) may serve as a guide which reflects the temperature dependence of the coordinate shifts due to the deformation. The structural PT in  $\text{HNb}_6\text{I}_{11}$  at 324 K is similar to the PT for  $\text{Nb}_6\text{I}_{11}$  described above. Figure 3(b) shows  $\sqrt{I}$  vs  $T$  for this compound. The temperature dependence of  $\sqrt{I}$  may be approximated by Eq. (1) with the exponent  $\beta=0.1$  and  $T_s=120$  K.

### III. THERMAL AND MAGNETIC MEASUREMENTS

#### A. Specific-heat measurements

Definite confirmation of a phase transition in  $\text{Nb}_6\text{I}_{11}$  and  $\text{HNb}_6\text{I}_{11}$  came from the specific-heat mea-

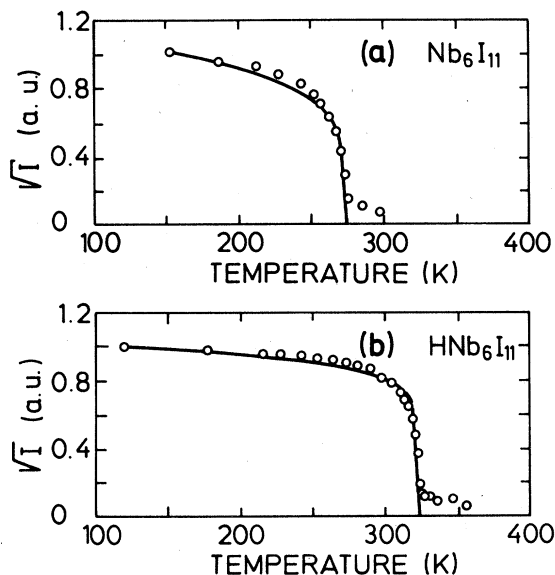


FIG. 3.  $\sqrt{I}$  vs  $T$  for  $\text{Nb}_6\text{I}_{11}$  (a) and  $\text{HNb}_6\text{I}_{11}$  (b). The solid line is the curve of Eq. (1). Note at  $T_c$  a rapid change in intensity.

surements. The specific heat of  $\text{Nb}_6\text{I}_{11}$  powder was measured between 150 and 400 K. A sharp peak appears at  $T=274$  K [see Fig. 4(a)]. This peak has the shape characteristic of a second- or higher-order PT.

The specific heat of  $\text{HNb}_6\text{I}_{11}$  was measured in the temperature interval  $150 < T < 450$  K, and the results are shown in Fig. 4(b). Two peaks appear in this curve. The peak at 324 K has a form similar to the peak seen in  $\text{Nb}_6\text{I}_{11}$ , but with a larger height and a more pronounced low-temperature wing. This low-temperature peak corresponds to the structural phase transition.

The other peak in the specific-heat curve of  $\text{HNb}_6\text{I}_{11}$  at 385 K has an almost symmetrical shape. X-ray investigations show no structural changes in this region.<sup>13</sup> This peak is believed to be due to precipitates of  $\text{NbH}_x$  where  $0.7x < 0.9$ . It is known that  $\text{NbH}_x$  undergoes a PT from the  $\alpha$  phase to  $\beta$  phase in this temperature region.<sup>14</sup> The height and shape of this peak is very sensitive to sample preparation, also indicating an impurity origin.

Due to the combination of poor thermal conductivity, the powder grain size, and the dynamic nature of the measurement, the experimental error in heat capacity is approximately  $\pm 3\%$  for  $\text{Nb}_6\text{I}_{11}$  and  $\pm 5\%$  for  $\text{HNb}_6\text{I}_{11}$ . Because of this large error, a meaning-

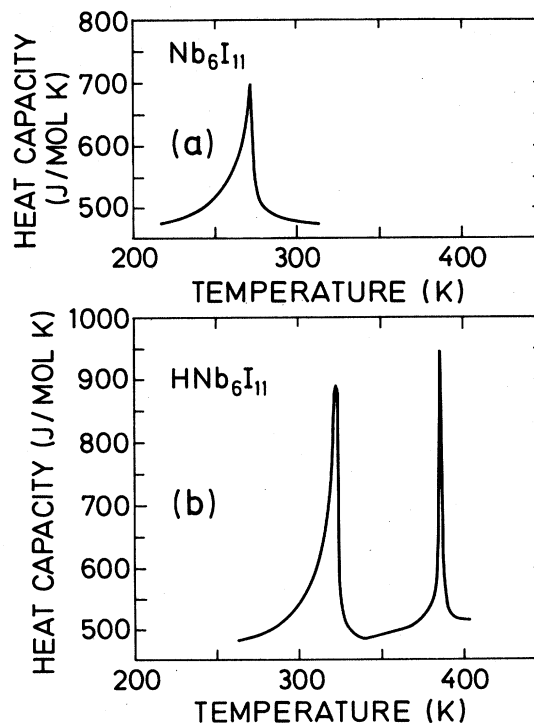


FIG. 4. Heat capacity vs  $T$ . The peaks at  $T=274$  K in  $\text{Nb}_6\text{I}_{11}$  (a) and  $T=324$  K in  $\text{HNb}_6\text{I}_{11}$  (b) correspond to the structural phase transitions indicated in Fig. 3. The peak at  $T=390$  K in  $\text{HNb}_6\text{I}_{11}$  (b) is due to precipitates of  $\text{NbH}_x$ .

ful analysis of the area under the heat-capacity peaks is not possible for these measurements. We note, however, that the peak at 324 K in  $\text{HNb}_6\text{I}_{11}$  is significantly larger than the corresponding peak at 274 K in  $\text{Nb}_6\text{I}_{11}$ . This is to be expected since the reduction of degeneracy is greater for  $\text{HNb}_6\text{I}_{11}$  (from a triplet to a singlet) than for  $\text{Nb}_6\text{I}_{11}$  (from a quartet to doublet).

## B. Magnetic-susceptibility measurements

We report here new magnetic-susceptibility measurements performed on a Faraday balance in fields up to 10 kG. Each measurement was made on several  $\text{Nb}_6\text{I}_{11}$  single crystals and on  $\text{HNb}_6\text{I}_{11}$  powder samples. Powder was used to assure completely hydrogenated clusters. Because the powder is air sensitive, the  $\text{HNb}_6\text{I}_{11}$  samples were sealed under a pressure of 500-mm helium gas in high-purity quartz tubes.

### 1. $\text{Nb}_6\text{I}_{11}$

Figure 5(a) presents the inverse magnetic susceptibility between 10 and 700 K. The diamagnetic contribution of  $\chi_{\text{dia}} = -750 \times 10^{-6} \text{ cm}^3/\text{mol}$  (Ref. 6) has been subtracted from the experimental data. The  $\chi^{-1}$  curve may be divided into four regions. The simplest region to understand is between 40 and 170 K and may be described by the Curie-Weiss law supplemented by Van Vleck paramagnetism,

$$\chi = \frac{C}{T - \Theta} + \chi_{\text{VV}}^{\text{low}}, \quad (2)$$

$$C = g^2 \frac{S(S+1)\mu_B^2 N_a}{3k_B},$$

where  $\mu_B$  is the Bohr magneton,  $N_a$  is Avogadro's number,  $k_B$  is Boltzmann's constant, and  $\chi_{\text{VV}}^{\text{low}}$  is the low-temperature Van Vleck contribution. We find the parameters  $g = 2.45$ ,  $S = \frac{1}{2}$ ,  $\Theta = -40 \text{ K}$ , and  $\chi_{\text{VV}}^{\text{low}} = 640 \times 10^{-6} \text{ cm}^3/\text{mol}$  fit the experimental points. The temperature dependence of the Van Vleck contribution is not essential in this region. This shows that the upper energy levels here are situated considerably higher than 200 K. The justification for the Van Vleck contribution will be given later.

Region IV may be also crudely explained by Curie-Weiss behavior with a  $S = \frac{3}{2}$  ground level. It is also influenced by the gap between the ground and excited levels. The solid curve in Fig. 5(a) is drawn according to the theoretical Eq. (14) which takes into account the presence of the paramagnetism of the excited states and contains the actual exchange inter-cluster parameters.

Region III represents nontrivial and unusual

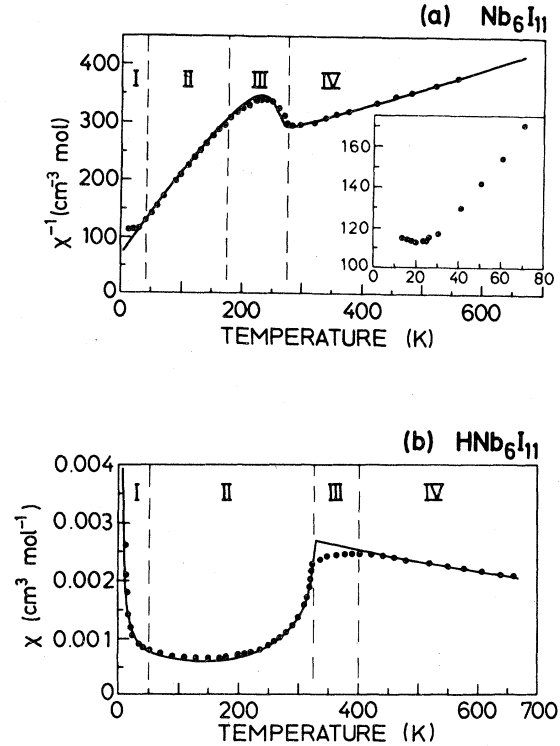


FIG. 5. Inverse susceptibility vs  $T$  for  $\text{Nb}_6\text{I}_{11}$  (a) and direct susceptibility vs  $T$  for  $\text{HNb}_6\text{I}_{11}$  (b). The diamagnetic contribution  $\chi_{\text{dia}} = -750 \times 10^{-6} \text{ cm}^3/\text{mol}$  has been subtracted from the data. The experimental error is approximately 3%. The solid lines represent the theoretical fitting of Eq. (14).

behavior of the magnetic susceptibility. It is clear that this behavior is connected with the structural PT at  $T_c = 274 \text{ K}$ . Indeed from Fig. 5(a) we see that at this temperature the inverse susceptibility changes rapidly. After reaching a maximum, the inverse susceptibility nears the Curie-Weiss behavior for the spin  $= \frac{1}{2}$  states.

This behavior may be understood qualitatively by the assumption that at  $T = T_c$  the level with higher spin ( $S = \frac{3}{2}$ ) crosses the level with the smaller spin ( $S = \frac{1}{2}$ ). As the temperature decreases, the depopulation of the  $S = \frac{3}{2}$  level, due to an increase in the separation between the two levels, makes the susceptibility smaller. When the energy gap between the two levels reaches a large value, the main contribution to the susceptibility comes from the ground  $S = \frac{1}{2}$  level and the usual Curie-Weiss behavior occurs.

Region I in Fig. 5(a) still presents a puzzle. Ordinarily one would expect from the Curie-Weiss behavior in the second region onset of antiferromagnetism at  $T_N < |\Theta| \approx 40 \text{ K}$ . And indeed, at

$T_N \approx 20$  K a bond appears in  $\chi^{-1}$  [see insert of Fig. 5(a)]. But neither elastic neutron scattering studies nor our preliminary specific-heat measurements give any indication of an ordered state above a temperature of 2.5 K. As we mentioned in Sec. II, the main intercluster exchange interactions take place via the iodine ions. One set of interactions is along the diagonal ( $\pm a, 0, c$ ) directions and is labeled with an exchange constant  $J$ . The other set of interactions is between clusters in the ( $a, b, 0$ ) plane and we label this interaction  $J'$ . If  $J' \ll J$ , the system is effectively one dimensional and the actual 3d ordering would occur at a much lower temperature than  $\Theta$ .<sup>15</sup> In the opposite case  $J' \gg J$ , the system is effectively two dimensional. Unfortunately, there is no theoretical estimation of the intercluster exchange and we do not know the true asymmetry between the exchange constants  $J$  and  $J'$ . We note only that according to the Nohl and Andersen estimation, the low-temperature phase of  $\text{Nb}_6\text{I}_{11}$  is characterized by an inhomogeneous distribution of electronic charge.<sup>9</sup> This in principle, may lead to a large anisotropy of the intercluster exchange interaction. But it remains to be established if the low-temperature magnetic properties are of a low-dimensionality nature.

## 2. $\text{HNb}_6\text{I}_{11}$

Qualitatively, the results reported here are, for the most part, similar to those in Ref. 7. However, there is one significant feature found here which was not seen in Ref. 7, namely, that between 324 and 400 K  $\partial\chi/\partial T > 0$ . The gross features of the susceptibility are the transition from the high-temperature paramagnetic Curie-Weiss behavior [region IV in Fig. 5(b)] to the diamagnetism of region II and further to the paramagnetic behavior for low temperatures in region I.

The low-temperature paramagnetic behavior in region I can be easily attributed to paramagnetic impurities. One possible source of paramagnetic impurities is unhydrogenated clusters. If we assume a  $S = \frac{1}{2}$ ,  $g = 2$  state for the impurity, this leads to a concentration of 5% of unhydrogenated clusters. Another possible impurity is  $\text{NbH}_x$ . When the impurity contribution is subtracted from the susceptibility, this leaves a temperature-independent part of

$$\chi_{\text{TI}} = -180 \times 10^{-6} \text{ cm}^3/\text{mol} \quad (3)$$

Because the diamagnetic contribution is approximately  $-750 \times 10^{-6} \text{ cm}^3/\text{mol}$  (Ref. 6) we conclude that the low-temperature Van Vleck contribution is about

$$\chi_{\text{VVO}} = +570 \times 10^{-6} \text{ cm}^3/\text{mol} \quad (4)$$

This value is in good agreement with recent calcula-

tions by Nohl and Andersen which give  $\chi_{\text{VVO}} = 500 \times 10^{-6} \text{ cm}^3/\text{mol}$  in the low-temperature phase, and earlier investigations.<sup>6</sup> The susceptibility in the fourth region is only approximately a Curie-Weiss curve. However, for a good fitting of experiment to theory, the paramagnetism of the excited states and temperature dependence of Van Vleck terms are important and the refined fitting is described in Sec. IV B.

The most peculiar behavior is in regions II and III. Note that at 324 K where the structural PT occurs, the susceptibility starts to decrease very abruptly as the temperature is lowered. It is clear that the system loses its paramagnetism and becomes diamagnetic for  $T < 150$  K. This process may be described in full analogy with the  $\text{Nb}_6\text{I}_{11}$  compound by the triplet-singlet level crossing.

Region III is more puzzling. In this region the derivative  $\partial\chi/\partial T > 0$  but in contrast to the second region, the derivative is small. The x-ray data do not show any changes in the symmetry and the form factors,<sup>13</sup> and there are no significant changes in the atomic coordinates.

One possible explanation for the magnetic behavior in region III is antiferromagnetic ordering. This order then is destroyed by the triplet-singlet level crossing. Neutron scattering measurements, with  $\lambda = 2.5$  Å, showed no evidence for magnetic order.<sup>16</sup> Extending neutron scattering measurements to longer wavelengths and measurements of the magnetic susceptibility on oriented single crystals would be interesting.

The other possible explanation for the behavior in region III would involve small shifts in the energy of the upper levels. The level movements would have to be accompanied by a change of the charge distribution and therefore have to manifest itself in the x-ray intensities. No large changes are seen in the x-ray patterns in this temperature range. However, if the level shifts are small, the changes in the x-ray patterns might be undetectable, and thus we cannot rule out this possibility.

## IV. THEORY

### A. Electronic structure

We present here the main results of the electronic-structure calculation by Nohl and Andersen.<sup>9,17</sup> The calculation by Nohl and Andersen used as input only the coordinates of the cluster ions. The x-ray study<sup>8</sup> gives the configurations for each compound both above and below the structural PT. From the calculated one-electron energy levels, the energy of the ground and several excited states were constructed for both high and low temperatures. Figure 6 represents the results of the Nohl and Andersen cal-

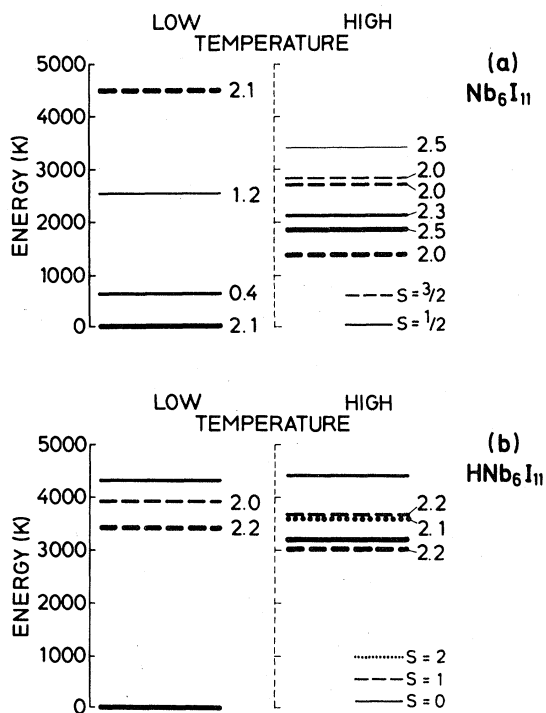


FIG. 6. Molecular-orbital calculation of energy levels in the high- and low-temperature phase of  $\text{Nb}_6\text{I}_{11}$  (a) and  $\text{HNb}_6\text{I}_{11}$  (b). The numbers indicate the calculated  $g$  values for the different levels.

calculation for high ( $\text{Nb}_6\text{I}_{11}$   $T = 298$  K,  $\text{HNb}_6\text{I}_{11}$   $T = 347$  K) and low ( $\text{Nb}_6\text{I}_{11}$   $T = 110$  K,  $\text{HNb}_6\text{I}_{11}$   $T = 216$  K) temperature phases.

The main result of the electronic-structure calculations from our point of view is the confirmation of the fact that the electronic degeneracy is reduced in  $\text{Nb}_6\text{I}_{11}$  and removed in  $\text{HNb}_6\text{I}_{11}$  via the level crossing. Concerning the calculated values of the gaps between the ground state and excited states, one would expect that because of the non-self-consistent nature of the calculations and the presence of correlation effects the actual numbers may be somewhat different.

In the high-temperature region  $T > T_c$  the changes in atomic positions with temperature are unimportant. Below the structural PT the main deformation is a twist as mentioned before. One may estimate the intermediate atomic positions just by linear interpolation of the between  $T_c$  and  $T_s$ . Using this method, Nohl and Andersen calculated the energy levels for intermediate positions and found that they move approximately linearly with the distortion.

#### B. Application of the two-level model with a crossing to magnetic susceptibility

The noninteracting cluster picture cannot explain the experimental results presented in Fig. 5. If we

use the theoretical level scheme, Fig. 6, including the calculated values for  $g$  factors and gaps, the susceptibility does not match the experimental results. We must therefore include a cluster-cluster exchange interaction. We expect that the iodine atoms provide the system with an indirect exchange coupling between the different clusters.

To perform actual calculations, the exchange constants between the various levels in Fig. 6 must be known. Because such information is absent, the use of the full energy-level scheme would introduce a large number of fitting parameters (exchange interactions for each pair of levels). To avoid this complication and to keep only the most essential features of the system, we propose here a two-level model with a crossing of these levels at  $T_c$ . We assume that the curve  $\sqrt{I}$  vs  $T$  (Fig. 3) is a good representation of the temperature dependence of Eq. (1) for the atomic coordinates for both compounds; it is possible to derive the temperature dependence of the energy levels of a cluster.

Figure 7 illustrates the main features of this model. For  $\text{Nb}_6\text{I}_{11}$  the two levels have, respectively,  $S_B = \frac{3}{2}$  and  $S_A = \frac{1}{2}$  and they are separated by a temperature-dependent gap,  $\Delta(T)$ , which takes the constant values  $\Delta_H$  above  $T_c$  and  $\Delta_L$  ( $< 0$ ) below  $T_s$ . In the transition region,  $\Delta(T) = \Delta_L \sqrt{I} + \Delta_H (1 - \sqrt{I})$ , where the temperature dependence of  $\sqrt{I}$  is the one given in Eq. (1). For the Van Vleck terms the theoretical values given by Nohl and Andersen are used.

We present the mean-field calculation below for our model. Let  $S_k$  and  $g_k$  be the spin and  $g$  factor for the ground level ( $k = 1$ ) and excited level ( $k = 2$ ). The contribution to the Langevin molar susceptibility from noninteracting clusters in level 1 is given by

$$\chi_1^0 = \frac{N_a \mu_B^2 g^2 S_1 (S_1 + 1) (2S_1 + 1)}{3k_B T Z(T)}, \quad (5)$$

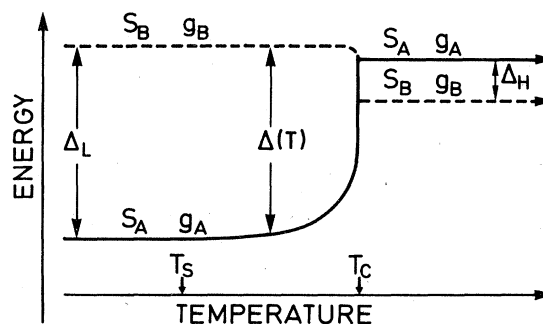


FIG. 7. Two-level model used for calculating the susceptibility. At high and low temperature the gap is constant. In the region of the phase transition, the gap is a function of temperature.

and the corresponding one for clusters in level 2 is

$$\chi_2^0 = \frac{N_a \mu_B^2 g^2 S_2 (S_2 + 1) (2S_2 + 1) e^{-\Delta/T}}{3k_B T Z(T)}, \quad (6)$$

where  $\Delta$  is measured in units of temperature and  $Z(T)$  is the partition function given by

$$Z(T) = 2S_1 + 1 + (2S_2 + 1) e^{-\Delta/T}. \quad (7)$$

In addition it is necessary to consider the Van Vleck contribution of the two-level model. This is given by

$$\chi_{VV} = \frac{N_a \mu_B^2 \alpha^2}{k_B \Delta} \left( \frac{1 - e^{-\Delta/T}}{Z(T)} \right). \quad (8)$$

Here,

$$\alpha^2 = \frac{2}{\mu_B^2 H^2} \sum_{mm'} |\langle 1m | H_Z | 2m' \rangle|^2 \quad (9)$$

is proportional to the square of the Zeeman interaction matrix elements between different states, where  $m$  and  $m'$  index the states of level 1 and 2. This expression is valid only when  $\Delta \gg g \mu_B H$  which will hold for the small fields considered here (away from the very near vicinity of the crossing).

We assume that the intercluster exchange interaction is of the Heisenberg scalar type. We need to include interactions between all the levels. We let  $\vec{S}_k^i$  be the spin of cluster  $i$  when it is in level  $k$ .

In these terms the interaction Hamiltonian between two spins on different clusters is

$$H_{\text{int}} = -J_{kk'}^i \vec{S}_k^i \cdot \vec{S}_{k'}^i, \quad (10)$$

where the three exchange constants  $J_{11}^i$ ,  $J_{22}^i$ , and  $J_{12}^i = J_{21}^i$  describe the possible exchange interactions between the  $i$ th and  $j$ th clusters.

We make the usual mean-field assumption that the thermal average  $\langle \vec{S}_k^i \rangle$  does not depend upon the cluster site  $i$ . Then one obtains for the average of the magnetization in level  $k$

$$\langle M_k \rangle = \frac{\text{Tr} \left( \frac{\partial \text{HMF}_k}{\partial H} e^{-\text{HMF}_k/k_B T} \right)}{\sum_k \text{Tr} (e^{-\text{HMF}_k/k_B T})}, \quad (11)$$

where

$$\begin{aligned} \text{HMF}_k = & \Delta_k - g_k \mu_B \bar{H} \cdot \vec{S}_k^i - \sum_{k'} J_{kk'}^i(0) \vec{S}_k^i \cdot \langle \vec{S}_{k'}^i \rangle \\ & + \sum_{k'} J_{kk'}^i(0) \langle \vec{S}_k \rangle \cdot \langle \vec{S}_{k'}^i \rangle, \end{aligned} \quad (12)$$

and

$$\Delta_1 = 0, \quad \Delta_2 = \Delta$$

and

$$J_{kk'}^i(0) = \sum_j J_{kk'}^{ij}. \quad (13)$$

After some algebra one obtains

$$\chi = \frac{\chi_1^0 + \chi_2^0 + (2\lambda_{12} - \lambda_{11} - \lambda_{22}) \chi_1^0 \chi_2^0}{1 - \lambda_{11} \chi_1^0 - \lambda_{22} \chi_2^0 + (\lambda_{11} \lambda_{22} - \lambda_{12}^2) \chi_1^0 \chi_2^0} + \chi_{VV} + \chi_{\text{dia}}. \quad (14)$$

The mean-field constants have their usual meaning

$$\lambda_{kk'} = \frac{J_{kk'}^i(0)}{g_k g_{k'} \mu_B^2 N_a}. \quad (15)$$

Equation (14) reduces to the usual mean-field expression if  $\chi_2^0 = 0$ .

One expects away from near vicinity of the crossing that the terms proportional to  $\chi_1^0$ ,  $\chi_2^0$  have only a very small contribution. Then Eq. (14) simplifies to

$$\chi = \frac{\chi_1^0 + \chi_2^0}{1 - \lambda_{11} \chi_1^0 - \lambda_{22} \chi_2^0} + \chi_{VV} + \chi_{\text{dia}} \quad (16)$$

in which the cross-exchange term has no contribution.

### 1. $\text{Nb}_6\text{I}_{11}$

We use Eq. (14) to fit the experimental points between  $T = 40$  and  $600$  K. At first sight we have a large number of parameters, i.e.,  $\vec{S}_k$  and  $g_k$ ,  $\Delta_L$ ,  $\Delta_H$ , three exchange constants ( $\lambda_{11}$ ,  $\lambda_{22}$ , and  $\lambda_{12}$ ), and the constant  $\alpha^2$  in the Van Vleck contribution. However, various regions of the susceptibility curve, Fig. 5(a), determine most of these parameters either unambiguously or within relatively narrow ( $\sim 10\%$ ) limits. The complete set of parameters used is shown in Table I.

The spins  $S_k$  for our model,  $S_1 = \frac{1}{2}$ ,  $S_2 = \frac{3}{2}$  below the PT and  $S_1 = \frac{3}{2}$  and  $S_2 = \frac{1}{2}$  above the PT, are an

TABLE I. Parameters used in calculation of susceptibility for  $\text{Nb}_6\text{I}_{11}$ . The Van Vleck parameters are taken from the calculations of Nohl and Andersen.

$S_A = \frac{1}{2}$	$g_A = 2.45$	$\Delta_L = -1400$ K
$S_B = \frac{3}{2}$	$g_B = 2.3$	$\Delta_H = 1000$ K
$\lambda_{11} = -70$	$\lambda_{12} = -70$	$\lambda_{22} = -265$
$\chi_{VV}^L = 640 \times 10^{-6}$ cm <sup>3</sup> /mol		
$\chi_{VV}^H = 800 \times 10^{-6}$ cm <sup>3</sup> /mol		

unambiguous choice. The  $g$  factors and exchange constants for the doublet ( $S = \frac{1}{2}$ ) and the quartet ( $S = \frac{3}{2}$ ) are fitted by the behavior in the Curie-Weiss regions II and IV, respectively. To be explicit, the slope may be directly related to the  $g$  factor and the temperature intercept related primarily to the appropriate exchange constant.

The bump region III is sensitive to the choice of the temperature-dependent gap  $\Delta(T)$  which is strongly dependent on  $\Delta_L$ . For the high-temperature region we set the gap  $\Delta_H$  equal to a constant. The susceptibility is not sensitive to the precise value of  $\Delta_H$  since the ground state in this region ( $S = \frac{3}{2}$ ) would have a factor 10 [due to the factor  $S(S+1) \times (2S+1)$ ] larger contribution to the susceptibility even if the population of the two levels were equal.

We comment briefly on the treatment of Van Vleck paramagnetism. Our model retains those levels that are the most important for the *Langevin* paramagnetism. The Van Vleck contribution comes from the mixing of all possible excited states due to the Zeeman term in the Hamiltonian. Within the framework of the present calculations it is not possible to single out the contribution of any excited level, so the effect of  $\Delta(T)$  on the Van Vleck contribution for the doublet quartet crossing cannot be calculated. We adopt here the approximation of considering  $\chi_{VV}^t$  constant under  $T_c$ , ignoring the expected small increase in the region  $\Delta \approx 0$ . In fitting the experimental points with our two-level model, we compensate this by having the excited quartet lie closer to the ground state. In this way, the value of  $\Delta_L$  reported here can be considered as a lower limit only. For high temperatures, we use our model directly. Equation (8) may be written

$$\chi_{VV}(T) = \chi_{VV}^t \frac{1 - e^{-\Delta_H/T}}{1 + (1/2)e^{-\Delta_H/T}}$$

In using this expression, we neglect the small thermal population of the higher levels not considered in our model. This overestimates slightly the actual value of  $\chi_{VV}(T)$ . As a result, the value of  $\Delta_H$  that is obtained from the fitting can be considered an upper limit. The Van Vleck parameters used here were taken from the calculations in Ref. 9.

The comparison of the theoretical curve with the experimental points in Fig. 5(a) shows that the model explains the magnetic behavior quite well. However, we have not tried to fit the behavior in region I. We feel that additional experimental and theoretical investigations are necessary in order to understand this behavior. As mentioned previously, one possibility here is low-dimensional behavior. Another possibility would be antiferromagnetic ordering but no such ordering has yet been seen by neutron scattering.

## 2. $\text{HNb}_6\text{I}_{11}$

The two-level scheme for  $\text{HNb}_6\text{I}_{11}$  is presented in Fig. 7. The levels have, respectively,  $S_B = 1$  and  $S_A = 0$ . The temperature dependence of the gap  $\Delta(T)$  and the Van Vleck paramagnetism are treated analogously to the case of  $\text{Nb}_6\text{I}_{11}$ .

We again use Eq. (14) but this time supplemented by the Curie law for the impurity contribution as discussed in Sec. III. The theoretical curve produced with the parameters listed in Table II is seen with the experimental points in Fig. 5.

The parameters are obtained in a similar manner to that used in the previous section, so we do not repeat the method here. As before a range of parameters of about 10% give equally good fittings.

The main difference between the theoretical curve calculated using Eq. (14) and the experimental points lies in the region between 324 and 400 K. We discussed in the previous section some possible causes for the magnetic behavior in this region.

We comment on the large  $g$  factor of 3.8 used in this model calculation. This is a result of neglecting the strongly magnetic  $S = 2$  level [shown in Nohl and Andersen's energy-level calculations Fig. 6(b)] in our two-level model. Inclusion of this level would reduce the  $g$  factor to approximately 2.3 and would also reduce the exchange constant  $J$ .

In conclusion we see that the two-level model systems, including exchange, give a good description of the experimental data. The model parameters are in reasonable agreement with those obtained from the molecular-orbital calculation, considering the level of accuracy of the latter and the oversimplification of the two-level model. Finally, it should be noted that common models, such as the *rigid* two-level model, cannot explain the behavior of the measured susceptibility.

We note that the parameters for the gaps, exchange constants, and  $g$  factors found in the model calculation should not be taken literally, as the "true" values for the system. The values for  $g_A$  and  $\lambda_{11}$  in  $\text{Nb}_6\text{I}_{11}$  should be quite accurate since in the low-temperature region other influences are small. However, the gaps and the exchange constants, will certainly be modified due to the other levels shown in Fig. 6 but which are ignored in this calculation.

TABLE II. Parameters used in calculation of susceptibility for  $\text{HNb}_6\text{I}_{11}$ .

$S_A = 0$		$\Delta_L = -1350$
$S_B = 1$	$g_B = 3.8$	$\Delta_H = 500$
$\lambda_{11} = -350$		
$\chi_{VV}^t = 570 \times 10^{-6} \text{ cm}^3/\text{mol}$		

## V. DISCUSSION

The most fascinating property of the  $\text{Nb}_6\text{I}_{11}$  and  $\text{HNb}_6\text{I}_{11}$  compounds is the existence of the structural phase transition accompanied by the crossing of the electronic levels. The evidence for this PT is seen in the experimental studies by x rays, and measurement of the specific heat and magnetic susceptibility.

It is a very interesting feature that the electronic levels are "soft" in the sense that they may be moved just by a change in temperature. One might speculate that pressure might also move the levels.

The model of the level crossing explains the magnetic susceptibility in most regions, but there are still two regions in which the behavior is unclear. In  $\text{Nb}_6\text{I}_{11}$  the region  $T < 40$  K still presents a puzzle. In  $\text{HNb}_6\text{I}_{11}$  the region  $324 < T < 400$  K is also not completely understood.

We outline some areas of experimental and theoretical research which we would expect to clear up the behavior in these regions.

*a. Phonons.* In general, all the phonon phenomena, including the expected softening of some optical modes (the twist deformation) has not been considered either from a theoretical or experimental viewpoint.

*b. Exchange.* A theoretical estimate of the exchange constants  $J$  for an interaction along a chain and  $J'$  for interactions within a plane would be very useful.

*c. NMR and ESR.* NMR on the protons (and on the nucleus of a cluster) may provide valuable information about charge densities. ESR could provide  $g$  factors and may be useful for an understanding of the region  $T < 40$  K in  $\text{Nb}_6\text{I}_{11}$ .

*d. Magnetic susceptibility on oriented single crystals.* This could give information on magnetic anisotropy and the possibility of ordering.

*e. Inelastic neutron scattering.* This would be a very powerful tool for the investigation of both the elec-

tron and the phonon properties. It is an urgent necessity to start inelastic neutron scattering measurements which may provide us with the gaps in the electronic level scheme and their temperature dependence as well as discovering the phonons responsible for the onset of the phase transitions at  $T_c$ .

*f. Raman spectroscopy.* This, in principle, may give a great deal of information about the gaps and phonons. Preliminary attempts were unsuccessful because the opaque character of the crystals resulted in burning of the samples. The problem is to choose a spectral interval in which the laser does not burn the crystal.

We hope that the richness of the physical phenomena in these cluster compounds will exceed the inconvenience caused by the lack of the geometrical symmetry and will attract serious attention from investigators.

## ACKNOWLEDGMENTS

The authors benefited from the continuous interaction with O. K. Andersen, H. Imoto, H. Nohl, and A. Simon. Three of us (R.C., E.V., and V.Z.) would like to thank P. Fulde for many discussions and constant interest in these investigations and for suggesting this project. One of us (J.F.) would like to thank A. Simon for suggesting the project, providing the original samples, and constant support of the experimental investigations. We are indebted to von Schnering for the introduction to the chemistry of cluster compounds, G. Lamprecht for providing single crystals, H. Imoto for providing the powder samples, and C. Riekel for assistance with the neutron scattering measurements at the Institute Laue-Langevin. We would like to thank the Max-Planck-Institut and especially P. Fulde and A. Simon for their hospitality.

\*Permanent address: Departamento de Física, Facultad de Ciencias, Universidad de Concepción, Concepción, Chile.

†Permanent address: Racah Institute of Physics, The Hebrew University of Jerusalem, Israel.

<sup>1</sup>H. Schäfer and H. G. von Schnering, *Angew. Chem.* **76**, 833 (1964); A. Simon, *Inst. Phys. Conf. Ser.* **39**, 353 (1978).

<sup>2</sup>A. Simon, *Angew. Chem.* (in press).

<sup>3</sup>For reviews, see, Ø Fischer, *Appl. Phys.* **16**, 1 (1978); K. Yvon, in *Current Topics in Materials Science*, edited by E. Kaldis (North-Holland, Amsterdam, 1979), Vol. 3.

<sup>4</sup>J. J. Finley, H. Nohl, E. E. Vogel, H. Imoto, R. E. Camley, V. Zevin, O. K. Andersen, and A. Simon, *Phys. Rev. Lett.* **46**, 1472 (1981).

<sup>5</sup>L. R. Bateman, J. F. Blount, and L. F. Dahl, *J. Am. Chem. Soc.* **88**, 1082 (1966).

<sup>6</sup>A. Simon, H. G. von Schnering, and H. Schäfer, *Z. Anorg. Allg. Chem.* **355**, 295 (1967).

<sup>7</sup>A. Simon, *Z. Anorg. Allg. Chem.* **355**, 311 (1967).

<sup>8</sup>H. Imoto and A. Simon (unpublished).

<sup>9</sup>H. Nohl and O. K. Andersen, in *Proceedings of the Conference on Physics of Transition Metals*, Leeds 1980, *Inst. Phys. Conf. Ser.* (in press); and (unpublished).

<sup>10</sup>Such transitions from high-spin to low-spin states have been seen for single-ion systems. See, for example, E. König and K. Madeja, *Chem. Commun.* **3**, 61 (1966); E. König and S. Kremer, *Theor. Chim. Acta.* **20**, 143

- (1971); R. Wöhl and K. Bärner, *J. Magn. Magn. Mater.* 21, 80 (1980); V. G. Bhide, D. S. Rajoria, G. Rama Rao, and C.N.R. Rao, *Phys. Rev. B* 6, 1021 (1972).
- <sup>11</sup>A review of the cooperative Jahn-Teller effect may be found in G. A. Ghering and K. A. Ghering, *Rep. Prog. Phys.* 38, 1 (1975).
- <sup>12</sup>J. J. Finley, E. Gmelin, and A. Simon, *Verhandl. DPG* 15, 263 (1980); W. Bauhoffer (private communication).
- <sup>13</sup>H. Imoto (private communication).
- <sup>14</sup>T. Schober and H. Wenzl, in *Hydrogen in Metals II*, edited by G. Alefeld and J. Vökl (Springer, Berlin, 1978), p. 32.
- <sup>15</sup>M. Steiner, J. Villain, and C. Windsor, *Adv. Phys.* 25, 87 (1976).
- <sup>16</sup>Some caution must be taken in evaluating the neutron scattering results in regard to the question of magnetic ordering. It is not clear what effect the extended nature of the cluster orbitals has on magnetic neutron scattering.
- <sup>17</sup>O. K. Andersen, W. Klose, and H. Nohl, *Phys. B* 17, 1209 (1978).